RF models of a cavity magnetron

Stanley Humphries, Ph.D.

Field Precision LLC
E mail: techinfo@fieldp.com
Internet: https://www.fieldp.com

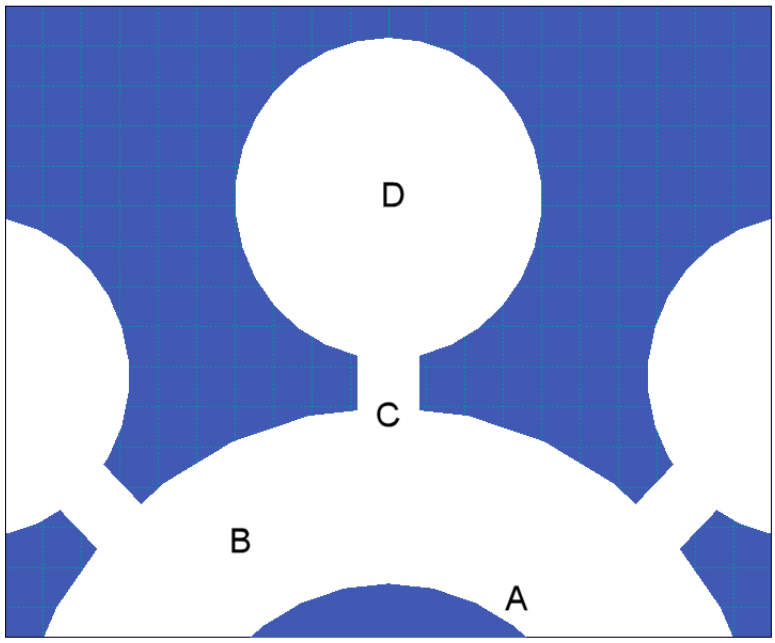

Figure 1: Cross-section of a cavity magnetron with eight cavities (detail)

The cavity magnetron is a widely-used source of high-power microwaves, from World War II radar to almost all microwave ovens. In this tutorial, I'll discuss the use of the 3D electromagnetic code **Aether** to find the resonant frequencies of a magnetron and to demonstrate the use of end-strapping to limit operation to a desired mode. Figure 1 illustrates the geometry. It shows a portion of the cross section of an eight-cavity structure, an extrusion of height H. We will associate the extrusion direction (out of the page) with the z axis of a three dimensional coordinate system. Electrons are emitted from a high-voltage cathode (A) and are pulled across the interaction region (B). Because of an applied axial magnetic field, the electrons cannot directly cross the gap but drift in the azimuthal direction. Cutouts in the grounded outer copper block define resonant cavities. The re-entrant shape of the cavities allows them to support a moderate frequency oscillation in a small structure. In the lowest order mode of a single cavity, an oscillating electric field drives current across the narrow gap (C). The current completes the circuit by flowing around the outer wall of the cylindrical chamber creating a magnetic field H_z. The gap (C) acts as a capacitor and the chamber (D) acts as an inductor, creating a resonant circuit. The azimuthal electric fields extend into the interaction region, influencing the drifting electrons so that they strike inner portions of the block in phase to yield energy to the oscillation. The self-consistent electron motion is a complex collective

problem that must be approached with a particle-in-cell simulation. Here, I will address only the RF portion of the calculation.

I will pick a specific geometry, but build it in a way that would allow easy changes for other systems. The height of the block is $H = 8.0$ cm. A symmetry boundary in the middle can be applied to reduce the calculation time. In this case, the block extends from 0.0 to 4.0 cm in z. The eight inductive cutouts are cylinders of radius $R = 1.0$ cm with center displaced 3.8 cm from the axis. The capacitive slots have gap width $D = 0.4$ cm and length $L \approx$ 0.35 cm. The interaction region has inner radius 1.4 cm and outer radius 2.5 cm. To set a starting point of the RF calculation, I made an estimate of the resonant frequency of a single cavity approximating fields as uniform in z. The capacitance of the gap is about

$$C \cong \epsilon_0 \frac{(2L)H}{D}. \tag{1}$$

The value 2 is a fudge factor to account for the energy of fringe fields around the narrow gap. Approximating the cylindrical chamber as a solenoid, the inductance is about

$$L \cong \mu_0 \frac{\pi R^2}{H}. \tag{2}$$

The single-cavity resonant frequency is

$$f = \frac{1}{2\pi\sqrt{LC}} \cong \frac{1}{2\pi\sqrt{\mu_0\epsilon_0\pi R^2(2L)/D}} \tag{3}$$

independent of the block height H. Inserting values for the test geometry, the frequency is $f_0 \cong 2$ GHz.

The cavities do not act independently, but are part of a periodic coupled structure. The RF oscillations are connected by shared electric fields in the interaction regions and shared magnetic fields at the top and bottom of the block. The coupled resonances would be difficult (if not impossible) to describe analytically, so a numerical calculation is required. Modes in a coupled structure are characterized by the oscillation phase differences in the individual components. The constraint is that the field quantities must repeat after eight components. We can express the axial magnetic field in the inductive region as

$$H_z = \cos(n\Delta\phi), \qquad n = 0, 7 \tag{4}$$

with the periodicity condition $1 = \cos(8\Delta\phi)$. The allowed values are

$$\Delta\phi = 0,\ \pi/4,\ \pi/2,\ 3\pi/4,\ \pi. \tag{5}$$

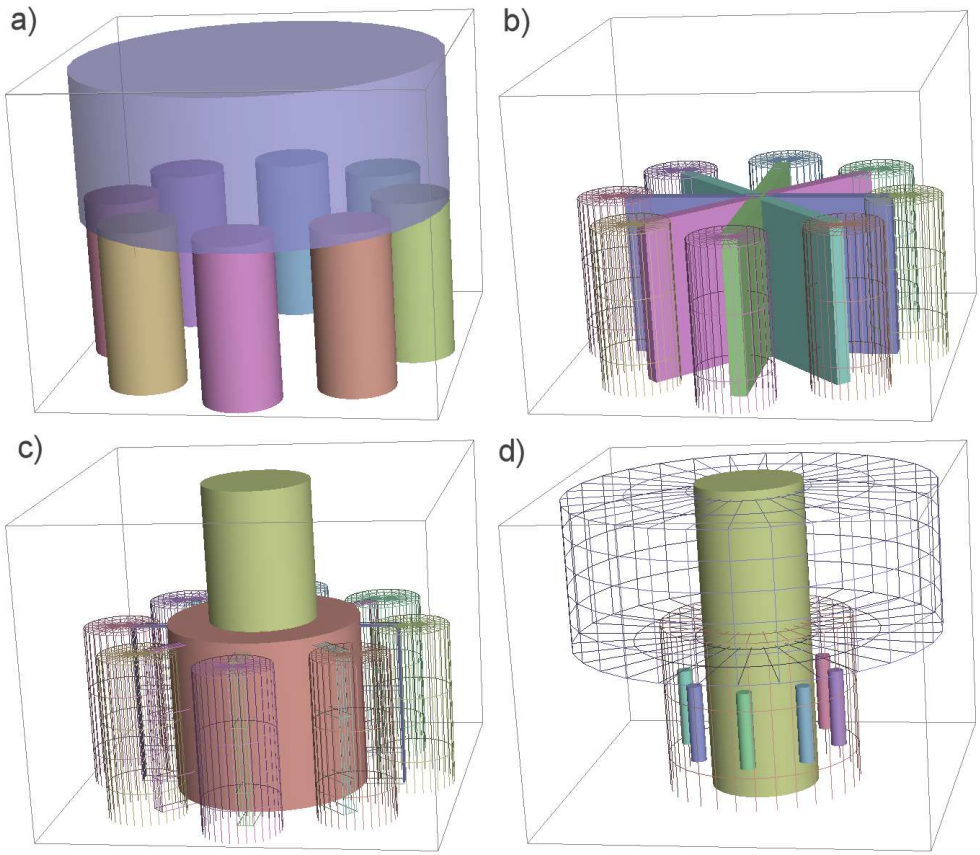

Figure 2: Steps in the construction of the mesh with **Geometer**.

The value $\Delta\phi = \pi$ gives the strongest electron interaction and the highest efficiency, so the goal is ensure that the system operates in that mode.

The geometry is fairly complex, so I will summarize the steps in building the mesh using the **Geometer** and **MetaMesh** components of the **Aether** suite. Although I used a symmetry boundary at the midplane in z, I represented the complete system in the x-y plane to allow multiple models and to investigate the effect of end straps. Figure 2 shows the steps in creating the mesh specification. There were two main regions of material: vacuum and copper. All copper parts were set to ground potential because the static voltage between the cathode and anode does not affect the RF solution. The solution volume covered the region -5.0 cm $\leq x, y \leq$ 5.0 cm and 0.0 cm $\leq z \leq$ 8.0 cm. The first part to add was a box with the properties of copper that filled the entire solution volume (the outline in Fig. 2a). The next step was to define the top of the block and the end space by adding a cylinder of radius 4.0 cm and length 3.8 cm (blue) with the material properties of vacuum. The shape over-wrote the previous material property of copper for the included

elements. In the default position, the cylinder extended between $z = \pm 1.9$ cm. After a shift $\Delta z = 5.9$ cm, the part extended between 4.0 cm $\leq z \leq$ 7.6 cm, defining a closed void above the block. The first cavity was a cylinder with vacuum properties of radius 1.0 cm and length 8.0 cm displaced 3.8 cm in x. The portion of the cylinder outside the solution volume was ignored by the codes. The other seven cavities were identical, except with different x-y shifts (in 45° increments). The operation could be performed within **Geometer** by duplicating the part and editing its shifts. Alternatively, the original part could be copied and pasted in the **MetaMesh** input script with the shifts modified with a text editor.

The next step (Fig. 2b) was to add the connecting slots to the interaction regions. The first slot (blue) was a box with dimensions $L_x = 7.0$ cm, $L_y = 0.4$ cm and $L_z = 8.4$ cm. It overlapped a small distance into the first and fifth cavities and extended across the central region. Two more such shapes were added with rotations of 45° and 90° as shown. The next step (Fig. 2c) was to carve out the interaction region, a cylinder of radius 2.5 and length 8.0 cm with vacuum properties. I then added the cathode, a cylinder of radius 1.4 cm with copper properties that extended the length of the solution volume. The mesh was completed by adding small cylinders with the material properties of vacuum that would carry drive currents to excite the RF oscillation in **Aether** (Fig. 2d). Each source had its own region number to allow assignment of specific current directions. The sources were cylinders with radius 0.2 cm and length 2.0 cm. They were shifted 2.0 cm in z, with x and y shifts to place them at a radius of 2.0 cm at 45° intervals.

Figure 3 shows the mesh generated by **MetaMesh** from the input specifications. With an element resolution of 0.1 cm, the mesh contained 800,000 elements. The procedure described used the basic combinatorial solid geometry capability of **Geometer** and **MetaMesh**. Alternatively, the programs could accept geometric information from 3D CAD programs in the form of STL files. The main advantage of the solid geometry approach is that it generates a parametric model of the geometry that is accessible to the user as a text file. For example, one entry for a part in the file appears as

```
PART
  Region: AIR
  Name: CAVITY1
  Type: Cylinder
  Fab:   1.00000E+00  8.40000E+00
  Shift:   3.80000E+00  0.00000E+00  0.00000E+00
END
```

The data could be copied, pasted and modified in a text editor to create multiple cavities. Find and replace operations could be used to make quick

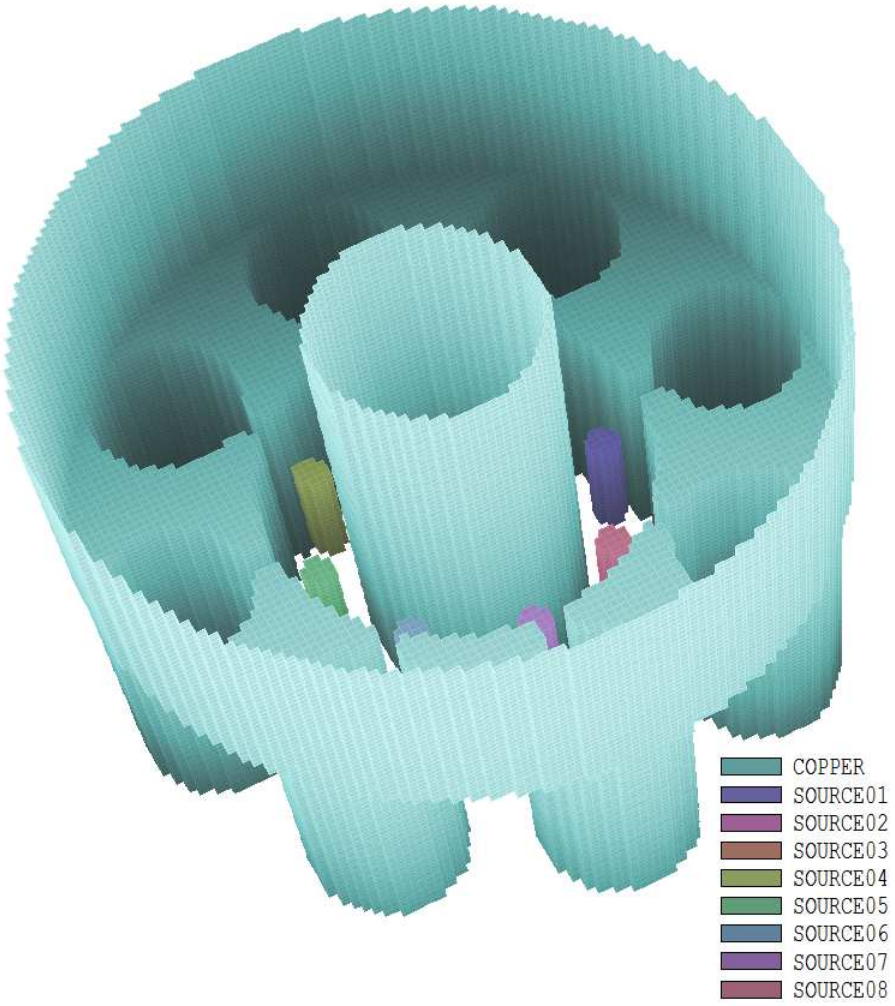

Figure 3: Completed mesh with the end plate at top removed.

global changes to the geometry. Optionally, **MetaMesh** could be called as a background **Windows** task with properties specified as pass parameters in a batch file. In this way, a range of geometries could be investigated automatically.

With the mesh completed, I turned to the RF calculations using the resonance and RF modes of **Aether**. The first step was a resonance search over broad frequency range centered near $f_0 = 2.0$ GHz. To emphasize the π mode, I assigned azimuthal current density to the eight source regions, alternating counter-clockwise and clockwise. The copper region was defined as metal ($\epsilon_r = 10^6,\ \mu_r = 10^{-6}$) and all other regions had the property of vacuum ($\epsilon_r = 1,\ \mu_r = 1$). In the resonant mode, **Aether** excites a time-domain solution by driving the sources with a pulse whose Fourier transform is a rounded step function with a specified central frequency and frequency width. I set the code to monitor the variation of H_z in the first cavity over several RF periods. At the end of the run, the code takes a Fourier transform of the probe signal. The initial run showed activity near 1.7 GHz. I then made a detailed run with $f_0 = 1.7$ GHz and $\Delta f = 0.5$ Ghz. A narrow frequency band requires an extended run time. With 4-core parallel processing, the calculation ran about 17 minutes. The run yielded the plot of Fig. 4a which clearly shows the presence of multiple modes. The program also provides a detailed analysis of the probe signal using a peak-fitting routine. The three peaks corresponded to frequencies 1.653 GHz, 1.673 GHz and 1.692 GHz.

Next, I set up **Aether** solutions in the RF mode to associate the frequencies with modes. In this mode, the program determines a frequency-domain solution by running a time-domain solution to equilibrium and then converting the field values to phasor form. The waveforms for drive currents are time-modulated harmonic functions at a single frequency. Calculations in the RF mode run quickly, in this case about 2-3 minutes. The calculation at $f_0 = 1.653$ GHz gave the result shown in Fig. 5a. The figure, a cross-section in a plane normal to the axis, plots H_z at an axial position near the block center at a reference phase of 20º . The color coding indicates almost a pure $\Delta\phi = \pi/2$ mode. A similar plot for $f_0 = 1.692$ corresponded to the $\Delta\phi = \pi$ mode. In this case there were significant variations of field amplitude between cavities, indicating the presence of other modes.

The process of strapping is used in magnetrons to encourage the preferential excitation of the $\Delta\phi = \pi$ mode. The idea is to add structures at the ends of the block that enhance inductive and capacitive coupling between the resonant cavities. Figure 6 shows the modified mesh geometry with a single-ring end strap. The circular strap was connected to only odd-numbered segments of the block. This connection method reduced the frequency of the pi mode and raised that of the other modes. With increased frequency separation, I

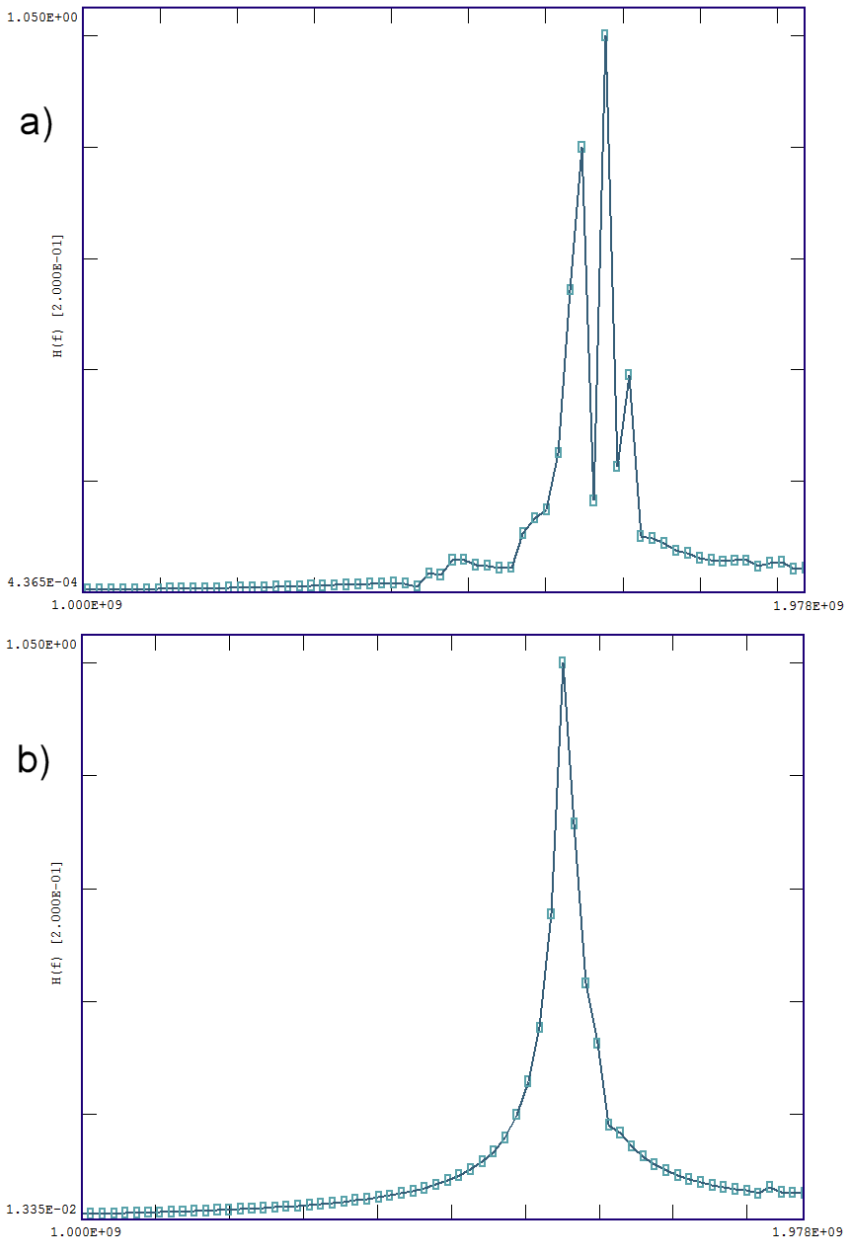

Figure 4: Frequency spectra for a resonance mode calculation. a) No strapping. b) With strapping.

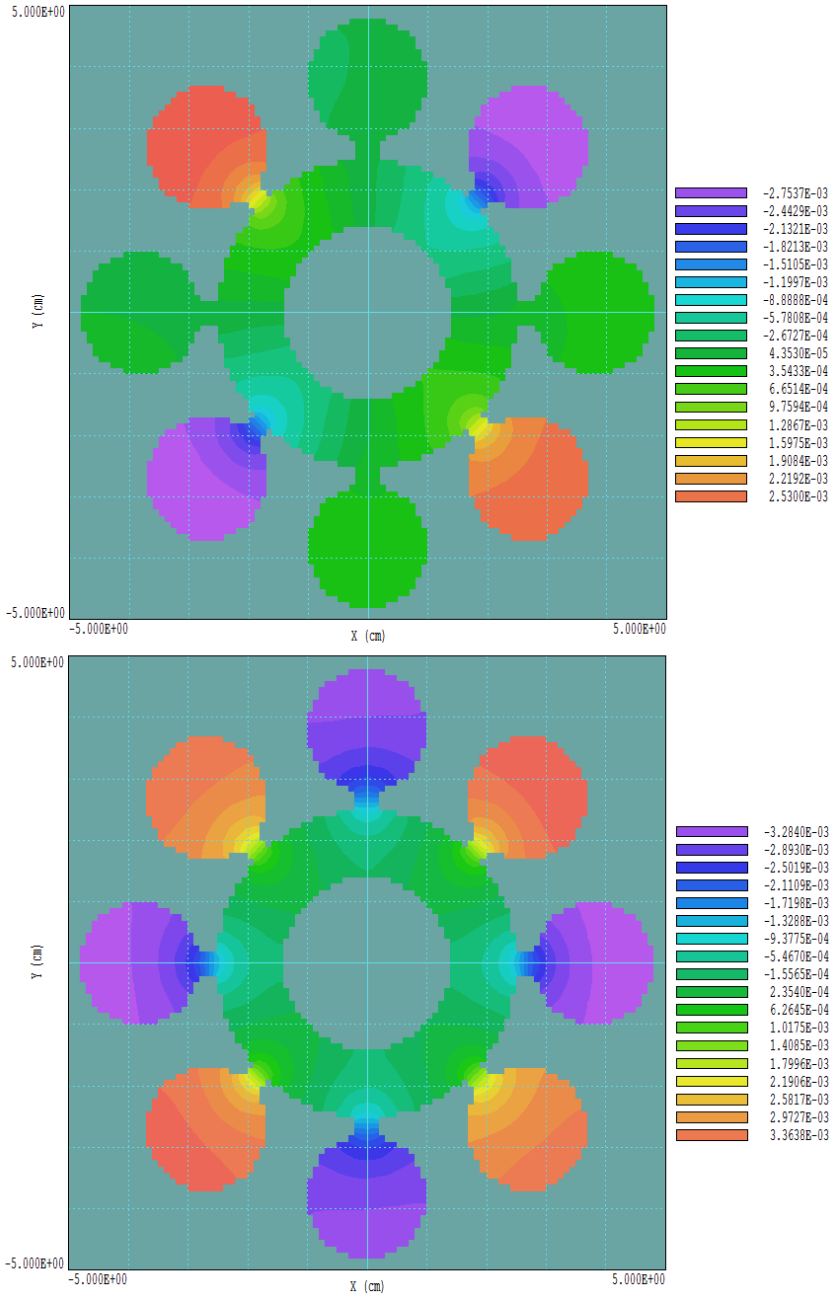

Figure 5: Plots of H_z in the plane $z = 2.0$ cm at a reference phase $\phi = 20^o$. a) $f_0 = 1.653$ GHz, no strapping. b) $f_0 = 1.652$ GHz, with strapping.

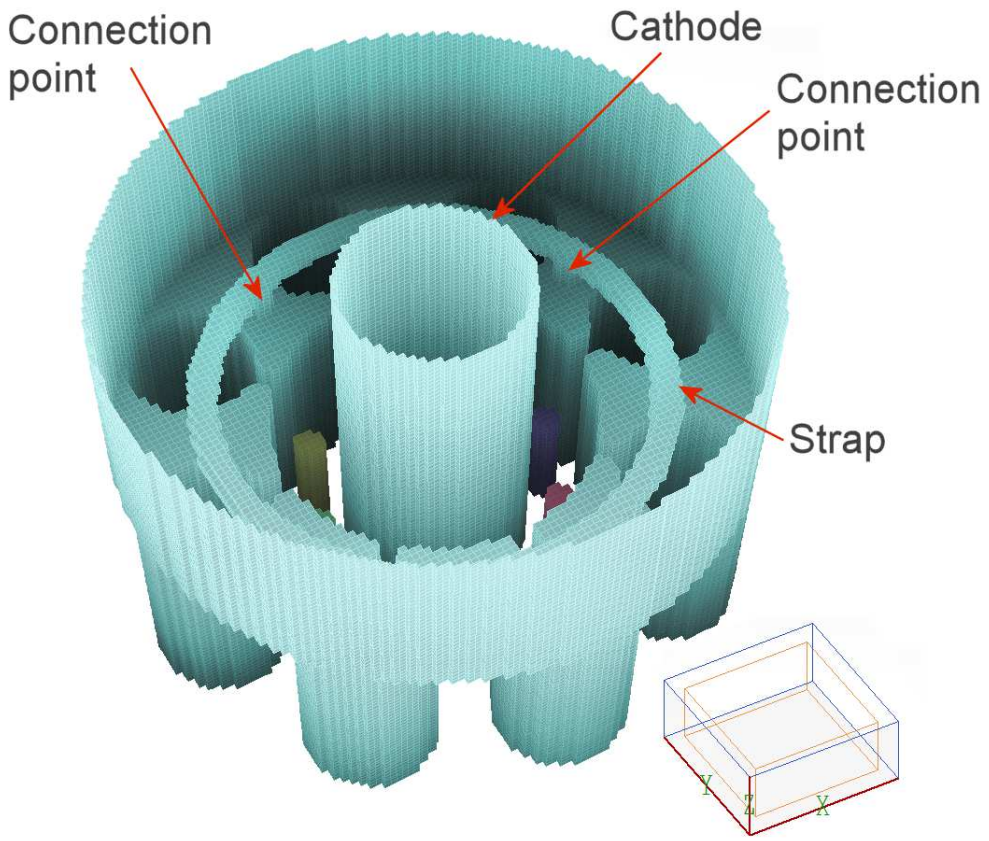

Figure 6: Single ring end strap added to the mesh.

expected that the alternating azimuthal currents of the sources will excite only the $\Delta\phi = \pi$ mode. Figure 4b shows the results of a resonant mode calculation with the modified geometry. There was a single resonance at 1.652 GHz with very little additional activity. A run in the RF mode at this frequency yielded the result of Fig.5b. The values of $|H_z|$ were almost identical in all cavities, indicating a pure $\Delta\phi = \pi$ excitation.

I would like to thank Scott Best of SiberSci LLC for suggesting this calculation.